THE X-LINKED INHIBITOR OF APOPTOSIS REGULATES LONG-TERM DEPRESSION AND LEARNING RATE

Julien Gibon[1,2], Nicolas Unsain[3], Karine Gamache[4], Rhalena A. Thomas[2], Andres De Leon[1,2], Aaron Johnstone[1,2], Karim Nader[4], Philippe Séguéla[2*], Philip A. Barker[1,2*]

[1]Vice Principal Research, University of British Columbia Okanagan campus, Kelowna, BC, Canada.
[2]Montreal Neurological Institute, McGill University, Montreal, QC, Canada**.**
[3]Laboratorio de Neurobiología, Instituto de Investigación Médica Mercedes y Martín Ferreyra, INIMEC-CONICET, Universidad Nacional de Córdoba, Córdoba, Argentina.
[4]Department of Psychology, McGill University, Montreal, QC, Canada.

Correspondence
*Co-corresponding authors :
Philippe Séguéla : philippe.seguela@mcgill.ca
Montreal Neurological Institute
Dept. Neurology & Neurosurgery, McGill University
3801 University, Office 778
Montreal, QC, Canada H3A 2B4
Phone: (514) 398-5029
Fax: (514) 398-8106

Philip A. Barker : phil.barker@mcgill.ca
Dept Vice Principal Research
The University of British Columbia
FIP322, 3247 University Way
Kelowna, BC, Canada, V1V 1V7
Phone: 250-807-9582
Fax: 250.807.8001

Running title: XIAP regulates hippocampal LTD.

List of Abbreviation

ACSF: Artificial Cerebro-Spinal Fluid

AMPA: α-amino-3-hydroxy-5-methyl-4-isoxazolepropionic acid

CASP3: Caspase 3

DIV: Day In Vitro

IAP: Inhibitor Of Apoptosis

IEI: Inter-Event Intervals

LTD: Long Term Depression

mEPSC: mini Excitatory Post-Synaptic Currents

NMDAR: N-methyl-D-aspartate receptor

PPF: Paired-Pulse Facilitation

XIAP: X-linked Inhibitor of Apoptosis

Abstract

Hippocampal long-term depression (LTD) is an active form of synaptic plasticity necessary for consolidation of spatial memory, contextual fear memory and novelty acquisition. Recents studies show that caspases play an important role in NMDAR-dependent LTD and are involved in postsynaptic remodeling and synaptic maturation. In the present study, we examined the role of X-linked inhibitor of apoptosis (XIAP), a putative endogenous caspase inhibitor, in synaptic plasticity in the hippocampus. Analysis in acute brain slices and in cultured hippocampal neurons revealed that XIAP deletion increases caspase-3 activity, enhances AMPA receptor internalization and sharply increases LTD and significantly reduces synapse density. Importantly, in vivo behaviors related to memory were also altered in $XIAP^{-/-}$ mice, with faster acquisition of spatial object location and increased fear memory observed. Together, these results indicate that XIAP plays an important physiological role regulating sublethal caspase-3 activity within central neurons and thereby facilitates synaptic plasticity and memory acquisition.

Keywords: XIAP, Caspase3, hippocampus, AMPA internalization, synaptic activity

Introduction

Hippocampal long-term depression (LTD) is an active form of synaptic plasticity necessary for learning (1-3), consolidation of spatial memory (4) and contextual fear memory (5). NMDA receptor-dependent LTD is characterized by a decrease in the strength of synapses. The internalization of post-synaptic AMPA receptors (6) is responsible for the decrease of excitatory post-synaptic potential observed in regular LTD in hippocampal slices. The influx of calcium after the activation of NMDAR, the recruitment of serine/threonine phosphatases such as calcineurin/PP2B and PP1 and other proteins such as GSK3β (7), Rap1 (8) and p38 MAP kinase (8) all play well established roles in NMDAR-dependent LTD.

Recent studies have shown that proteins of the apoptotic machinery are necessary for NMDAR-dependent LTD (9, 10), with caspase-9 and caspase-3 playing crucial roles in postsynaptic remodeling, synaptic maturation and attention-related behaviors (11-14). During LTD, the BAD-BAX cascade is activated and a transient release of cytochrome *c* from mitochondria (9) ultimately induces the activation of caspases-3 that is necessary for AMPAR internalization (10). The caspase-3 activation that occurs during LTD is moderate and transient, in sharp contrast to the massive accumulation of active caspase-3 observed during apoptosis.

Here, we considered whether endogenous proteins that suppress caspase-3 play a physiological role in central neuron plasticity. The mammalian IAP family has eight members but only one of these, *X-linked Inhibitor of Apoptosis Protein* (XIAP), acts as a direct inhibitor of caspase-9 and caspase-3 (15). We have recently shown that XIAP can reduce caspase-3 activity in sensory axons undergoing developmental degeneration (16) but whether this protein impinges on central nervous system plasticity by regulating sublethal caspase activity remains unknown.

In this study, we hypothesized that XIAP functions to regulate NMDAR-dependent LTD. Consistent with this, we observed that the magnitude of LTD is much higher in XIAP null mice than wild-type littermates and that AMPAR internalization after NMDA treatment is increased in hippocampal neurons lacking XIAP. Furthermore, we observed that synapse number is reduced in primary culture of hippocampal neurons derived from $XIAP^{-/-}$ mice. We went on to test memory acquisition in $XIAP^{-/-}$ in two distinct cognitive assays and found that $XIAP^{-/-}$ mice learned faster than WT littermates. These data provide the first evidence that endogenous XIAP regulates LTD and memory acquisition *in vivo* and supports the hypothesis that XIAP regulates plasticity within hippocampal synapses.

Material and Methods

Animals

All experimental procedures were approved by the McGill University Animal Care Committee and were in compliance with the guidelines of the Canadian Council on Animal Care. XIAP$^{-/-}$ mice were previously described (17). CASP3$^{-/-}$ mice were obtained from the Jackson Laboratory (strain B6.129S1-Casp3tm1Flv/J). Animals were housed under standard conditions with a 12 h light/dark cycle and free access to water and food.

Behavior

Subjects

Mice (8-12 week-old male littermates) were handled for 3 days prior to the start of the behavioral experiments for habituation.

Rotarod test

Mice were placed on a rotating rod (IITC life Sciences, USA) and the time each mouse maintained its balance on the rod was recorded. First, the speed of the rotarod was maintained at 4 rpm for 2 min to serve as a habituation session. After a 5-min rest period, the mice were placed again on the rotarod and the speed was accelerated from 4 to 40 rpm over a 5-min period. This test was repeated 3 more times with 5-min intersession intervals.

Open field test

Mice were placed individually in the center of the open field (50 x 50 x 30 cm) and their behavior was recorded for a 10-min period. The floor of the open field was divided into 9 squares and the following parameters were measured: total number of squares entered (defined as four paws moving into a square) and total number of entries in center squares.

Contextual Fear Conditioning and Fear Extinction

Contextual fear conditioning consisted of a 2-min period of chamber acclimatation, followed by two presentations of a 2-s foot shock of 0.6 mA separated by 1 min. The mice were returned to their home cage 1 min after the last shock. After training, on day 2 and 3, the mice were placed again in the conditioning chamber for an extinction trial which consisted in placing the mice in the chamber for 15 min without any foot shock. On day 4, the mice were tested for contextual fear memory by placing them in the conditioning chamber for a 5-min period. For all tests, behavior was recorded and

analysed using FreezeView software (Actimetrics, USA). Freezing, the conditioned response indicating fear memory retention, was analyzed for each mouse at in 3 min interval for extinction sessions and as a 5-min trial for the test sesión. Data are expressed as the percentage of time freezing in each interval.

Object Location Task

On day 1, mice were habituated twice in the empty arena (50 x 50 x 30 cm) for 10 min (4-hr intersession interval). The training trials consisted of 10-min sessions of object exploration, twice daily for two days. Mice were tested 48 hours after the last training session for 10 min. For training, two objects were located in opposite sides of the arena. For the testing session, one object was moved to a corner. Preference for the novel location was determined as the ratio of the exploration time for the object at the novel location divided by the total time spent exploring the two objects. The percentage of novel exploration during training trials is defined as the percentage of training 1 (exploration time for both objects in training sessions 2, 3, or 4 over the exploration time for both objects in training 1).

Electrophysiology in hippocampal slices

Hippocampal slices were obtained from mice (4-8 weeks old) Briefly, mice were anesthetized with ketamine:xylamine cocktail (60 mg/kg) and perfused with ice-cold choline chloride-based artificial cerebrospinal fluid (ACSF) containing (in mM) : 110 choline-Cl, 1.25 NaH_2PO_4, 25 $NaHCO_3$, 7 $MgCl_2$, 0.5 $CaCl_2$, 2.5 KCl, 7 glucose, 3 pyruvic acid and 1.3 ascorbic acid, pH 7.4 bubbled with carbogen (O_2 95 %, CO_2 5%). Hippocampal sagittal sections were obtained using a VT1000 vibratome (Leica, Ontario, Canada) in the same choline chloride-based solution. The slices were allowed to settle at RT (22-24°C) in ACSF containing (in mM): 124 NaCl, 3 KCl, 26 $NaHCO_3$, 1 $MgSO_4$, 1.25 NaH_2PO_4, 10 glucose, 2 $CaCl_2$ for 1h before recording.

Field recordings were made in the CA1 area. Stimulating electrodes were placed in the Schaffer collateral-commissural pathway. To induce LTD, low frequency stimulation at 1 Hz was delivered over 900 s. The field recording pipettes (2-3 MΩ) were filled with NaCl 2 M. EPSP slope and amplitude were analyzed off-line using Clampfit 9.2.1.8 (Axon instruments).

For mEPSC recordings, tetrodotoxin (1 μM) and picrotoxin (100 μM) were added to the perfusion solution. Spontaneous activity was recorded during 5 min with the resting membrane potential held at -70 mV. Brain slices were perfused by gravity at a speed of 1-2 ml/min at 32-34°C using a TC-324B temperature controller (Warner Instruments LLC, Hamden, CT). Patch pipettes (5-

9 MΩ) were pulled on a Brown Flaming puller (P-97, Sutter Instruments, Novato, CA) using borosilicate glass electrode (Sutter Instruments). Gigaseals (> 5GΩ) were obtained by applying negative pressure. Electrical signals were amplified using an Axopatch 200B amplifier (Molecular Devices, Sunnyvale,CA), low-pass-filtered at 10 kHz, digitized at 10 kHz via a Digidata 1322A interface (Molecular Devices). Intracellular solution was composed of (in mM): 120 K-gluconate, 10 HEPES, 0.2 EGTA, 20 KCl, 2 $MgCl_2$, 7 diTrisP-Creatine, 4 Na_2ATP and 0.3 NaGTP, pH 7.3. mEPSCs were analyzed off-line with the software Mini-analysis (Synaptosoft inc.). Paired-pulse facilitation was recorded only in presence of picrotoxin, stimulus was 70% of the maximal response observed for each cell.

Active caspase pull-downs

For biochemical experiments hippocampal neurons were cultured on filters with astrocyte feeder layers following a protocol adapted from Unsain *et al*, JOVE 2014. Dissociated cortical neurons were seeded at high density (5 X 10^5 cells) and maintained for 12-15 DIV. After NMDA treatment (30 µM, 15 min at 37ºC), biotin-VAD-fmk (bVAD; Santa Cruz Biotechnology) was added to the cortical neuron cultures (10 µM final concentration) and incubated for 10 or 90 min to capture active caspases. Cell culture inserts were then washed twice with ice-cold PBS. Pure axonal and dendrite samples were obtained by cleaning away the top surface of the filter and extracting in RIPA lysis buffer (150 mM NaCl, 1% NP40, 0.5% deoxycholate, 0.1% SDS, 50 mM Tris pH 8), supplemented with protease inhibitors (Roche). After lysis, membranes from two filters were pooled. A 50 µl aliquot was set aside as an input control and the remainder was incubated 4 hours with streptavidin-agarose beads (Pierce) at 4 ºC to pull down active caspase-bVAD complexes. The beads were washed extensively, and bound proteins were eluted using sample buffer then analyzed by SDS-PAGE and western blot.

GluR2 internalization

AMPA receptor internalization assays were done essentially as described in (18). The anti-GluR2 antibody (2 ug/ml, clone 6C4, Millipore) was added to live hippocampal neurons in conditioned medium for 30 min at 37ºC. Cells were then treated for additional 15 min with NMDA 30 µM, washed with PBS and fixed in paraformaldehyde (PFA) 4%, sucrose 4%. Surface anti-GluR2 was labeled with anti-mouse Alexa 546 secondary antibody (Life technologies) applied at a dilution of 1:500. After methanol permeabilization, internalized anti-GluR2 was detected with anti-mouse Alexa 488 secondary antibody (Life technologies) applied at a dilution of 1:500.

Synaptosomes preparation

Synaptosomes from adult mouse neocortex were prepared by centrifugation as described in Huttner, 1983. Wild-type and XIAP-/- tissue was homogenized in 10 volumes of 20 mM HEPES pH 7.4 containing 320 mM sucrose with 10 strokes of a glass-teflon homogenizer at 900 rpm and centrifuged for 10 min at 800 x g to collect nuclei and large debris. Supernatant was removed and centrifuged for 10 min at 12000 x g, and the resulting pellet was resuspended in 15 volumes of homogenization buffer and subsequently centrifuged for 10 min at 14500 xg to collect the synaptosomal fractions. Subcellular fractions were analyzed in Western blot with antibodies directed against histone H3 (1:2000, Millipore), PSD95 (1:1000, Thermoscientific) and Actin (1:40,000, MP Biomedicals). Antibodies directed against caspase-3 (1:2000), caspase-9 (1:500) and caspase-6 (1:200) were obtained from Cell Signaling Technology. XIAP was detected with anti-RIAP3 (1:2000) kindly provided by Robert Korneluk (University of Ottawa). cIAP1 and 2 were detected with anti-RIAP1 (1:1000, Cedarlane).

Synapse quantification

Hippocampal neurons were cultured as described in (19) on poly-L-lysine coated coverslips co-cultured with an astrocyte monolayer for 15 days in vitro then fixed in 4% PFA and 4% sucrose in PBS for 30 min, washed in PBS then briefly permeabilized with methanol and washed again in PBS. After 30 min blocking (PBS, 2.5% BSA and 2.5% Goat serum) neurons were triple labeled with mouse anti PSD95 diluted 1:200 (Thermoscientific MA1-045), rabbit anti synapsin1 diluted 1:2000 (a gift from Peter McPherson, McGill University) and chicken anti MAP2A diluted 1:2000 (EnCor CPCA-MAP2) for 2 hours at room temperature in PBS with 1% BSA. Coverslips were extensively washed in PBS then incubated with secondary antibodies: goat anti mouse Alexa 488, anti rabbit Alexa 556 (Life technologies) or goat anti-chicken Alexa 633 (Jackson Labs) diluted 1/500 in PBS with 1% BSA for 1 hour at room temperature.

Image analysis and quantification

For dissociated hippocampal neurons, digital images were obtained using a Zeiss AxioObserver Z1 inverted microscope using a 40x objective and 1388 x 1040 pixel resolution (0.161 μm/pixel). For each experiment, images were acquired as a z-stack of 15-19 optical sections (0.3 μm step size) followed by deconvolution (constrained iterative method). Projections made of z stacks were used for image analysis with the NIH software ImageJ. Synaptic density quantification: for each image, the

threshold for each channel was defined as the mean pixel intensity for the entire image plus two standard deviations above the mean. A binary mask that included all pixels above this threshold was created for each channel. Regions of interest corresponding to neuronal somata were drawn manually and excluded from further analyses in all channels. From these images, co-localization analysis was performed with the RG2B plugin and regions of double co-localization larger than 2 pixels in size were defined as objects. To calculate synapse density, the number of objects was divided by the area of the neuronal processes as measured using the MAP2 area (minus the cell body).

Results

To address the hypothesis that XIAP regulates NMDAR-dependent LTD, we first isolated synaptosomes from wild-type and XIAP$^{-/-}$ mouse brain cortices and established by immunoblotting that XIAP and caspase-3 are present in this compartment (Figure 1A). We then assessed NMDA-dependent long term depression (LTD) induction in wild-type and XIAP$^{-/-}$ hippocampal slices; Figure 1B shows that low frequency stimulation evoked much stronger LTD in XIAP$^{-/-}$ mice than in littermate controls (28% decrease slope in WT vs 70% decrease slope in XIAP$^{-/-}$, $p < 0{,}001$).

The LTD observed in XIAP$^{-/-}$ slices was entirely reversed by zDEVD-fmk, a caspase-3/7 inhibitor (Figure 1C), suggesting that it was caspase-3 dependent. To confirm this, we first asked if LTD could be induced in hippocampal slices of CASP3$^{-/-}$ null mice; consistent with an earlier study (10), we found CASP3-/- slices were unable to undergo LTD. We then examined hippocampal slices derived from CASP3$^{-/-}$:XIAP$^{-/-}$ compound nulls and as above, found that LTD could not be induced (Figure 1D). Therefore, the enhanced LTD evoked in XIAP-/- hippocampal slices requires neuronal caspase-3 activity

To demonstrate that XIAP deletion increases caspase-3 activity in hippocampal neurons, we maintained primary hippocampal neurons *in vitro* for 18 days and then used a caspase trapping assay (16) to assess levels of active caspase-3 before and after NMDA treatment. Figure 2A shows that basal and NMDA-induced caspase-3 activity levels are elevated in XIAP$^{-/-}$ hippocampal neurons compared to their wild-type counterparts. Because synaptic caspase-3 activity induces local pruning of dendrites and spines (20) and LTD can cause synapse loss (2, 21), we determined whether XIAP depletion alters synapse numbers in hippocampal neurons maintained *in vitro* for 21 days. Figure 3A-C shows that XIAP$^{-/-}$ hippocampal neurons form significantly fewer synapses than their littermate controls within this time frame.

We then went on to measure spontaneous mini excitatory post-synaptic currents (mEPSC) in hippocampal slices and found significantly smaller amplitudes and longer inter-event-intervals (IEI) in slices derived from XIAP$^{-/-}$ mice (Figure 4A-C). However, paired-pulse facilitation was unaffected by XIAP deletion (Figure 4D) and therefore defects in synaptic activity in XIAP$^{-/-}$ mice likely reflect alterations in the post-synaptic compartment.

Long term depression elicited by repetitive electrical stimulation or by NMDA treatment normally results in the internalization of AMPA receptors on hippocampal CA1 neurons. To test whether the enhancement of LTD observed in XIAP$^{-/-}$ slices is accompanied by increased AMPA receptor internalization, we examined NMDA-dependent GluR2 internalization in hippocampal neurons derived from XIAP$^{-/-}$ animals or age-matched controls. Figure 5A and B show that NMDA-

dependent AMPAR internalization is significantly, albeit modestly, increased in XIAP$^{-/-}$ hippocampal neurons.

Hippocampal LTD is an active form of synaptic plasticity necessary for consolidation of spatial memory (4) and contextual fear memory (5) and we therefore tested the behaviour of XIAP$^{-/-}$ mice in several memory tasks. XIAP$^{-/-}$ mice were indistinguishable from wild-type animals on rotarod and open field tests (Figure 6A-B), suggesting that their motor coordination and anxiety levels are normal. To determine if the enhanced LTD present in XIAP$^{-/-}$ improves performance in LTD-related tasks, XIAP$^{-/-}$ mice were tested in a novel object location test. Interestingly, XIAP$^{-/-}$ mice displayed faster acquisition, significantly outperforming wild-type littermates at early training sessions (Figure 6C-D). However, 48 hours after training, performance was not significantly different between the groups (Figure 6E-F). Similarly, during contextual fear extinction learning, freezing dropped significantly faster in XIAP$^{-/-}$ mice compared to wild-type littermates (Figure 6G) but 24 hours after the last extinction session, responses of the XIAP$^{-/-}$ and wild-type mice converged and were not significantly different. We conclude that deletion of XIAP results in more rapid acquisition of hippocampal-dependent behavioral tasks.

Discussion

In the present study we investigated the role of endogenous XIAP in regulating NMDA-dependent LTD, AMPA internalization, synaptic physiology, and memory-related behaviors in mice. We observed that XIAP is normally present at synapses, suggesting it may play a physiological role regulating caspase-dependent synapse modulation at central synapses. Consistent with this, using a low frequency stimulation protocol that produces NMDA-dependent LTD (2), we found that mice lacking XIAP undergo considerably stronger LTD than their wild-type littermate counterparts and that this effect of XIAP deletion was lost when caspase-3 was absent or when caspase-3 activity was blocked pharmacologically. Indeed, the fact that DEVD worked to recover the XIAP phenotype shows that the effect of XIAP is due to an acute regulation of caspase-3 and not due to a developmental deffect in slices from $XIAP^{-/-}$ mice. The germline deletion of XIAP could have also influence the level of caspase-9 and caspace-7 in the brain, however we show that DEVD and caspase-3 knockout produces the same phenotype (no LTD), this result strongly implies that DEVD normally acts to block caspase-3 in this context. From these data, we postulate that endogenous XIAP modulates synaptic transmission and that it does so by suppressing caspase-3 activity.

Previous studies have established that caspase-3 activation accelerates AMPA receptor internalization (4) and we therefore postulated that reducing XIAP level would increase NMDA-induced AMPA internalization. Consistent with this, we observed that internalization of GluR2 was increased in hippocampal neuron derived from XIAP null mice, compared to wild-type controls. Together, these results demonstrate that endogenous XIAP regulates the NMDA-dependent-internalization of AMPA receptor and influences long term depression in the hippocampus.

LTD is also associated with spine shrinkage and pruning (22, 23) and caspase activity seems to play a critical role driving these morphological changes (20). Consistent with this, we observed that XIAP null neurons form less synapses than WT neurons and found that spontaneous synaptic activity is reduced in brain slices from XIAP null mice. Our results on LTD and AMPA receptor internalization suggest that the effect on XIAP on central neuron activity reflects mainly a post-synaptic role. Consistent with this, paired-pulse recordings demonstrated that the release of glutamate is not affected by XIAP deletion.

It is clear that LTD is involved in memory acquisition and maintenance (Bliss and Collingridge, 1993) but the role of endogenous XIAP in memory tasks has not previously been investigated. We tested $XIAP^{-/-}$ mice for object location and fear memory and found that in both paradigms XIAP null mice learned faster than their wild-type littermates. Interestingly, a recent article showed that caspase-3 null mice do not differ in memory capabilities yet they display

increased impulsivity, impaired attention and reduced behavioral flexibility (14). XIAP null mice have increased rates of learning but as in caspase-3 null mice, memory retention is not altered. Taken together, these data reinforce the notion that sublethal caspase activity plays a crucial role in regulating synaptic activity and for the first time, demonstrates that XIAP plays a key in this process.

Of the eight IAP family members present in mammals, only XIAP is capable of directly blocking caspase-3 enzymatic activity (24-27). XIAP overexpression occurs in several types of human cancer and can facilitate cell survival in pathogenic gain-of-function circumstances (28) yet XIAP does not play a significant role regulating apoptosis under physiological circumstances. Indeed, it has proven suprisingly difficult to identify normal physiological circumstances in which XIAP regulates caspase-3 (29). Here, we demonstrate that XIAP normally regulates sublethal caspase-3 activity in the central nervous system and by doing so, exerts a profound effect on nervous system synaptic plasticity. These data suggest that a predominant physiological role for XIAP is in the sublethal regulation of synaptic caspase activity.

Conflict of Interest: none

Author and Contributors

J .G. designed experiment, performed experiments, analyzed the data and wrote the paper, N.U. designed experiment, performed experiments, analyzed the data and wrote the paper, K.G. performed experiments and analyzed the data, R.A.T performed experiments and analyzed the data, A.D.L. performed experiments and analyzed the data, A.J. performed experiments and analyzed the data, K.N. analyzed the data and wrote the paper, P.S. analyzed the data and wrote the paper, P.A.B. design experiment, analyzed the data and wrote the paper.

Funding:

This project was supported by research grants #130239 and #37850 from the Canadian Institutes of Health Research to PS and PAB, respectively.

References:

1. Bliss, T. V., and Collingridge, G. L. (1993) A synaptic model of memory: long-term potentiation in the hippocampus. *Nature* **361**, 31-39
2. Collingridge, G. L., Peineau, S., Howland, J. G., and Wang, Y. T. (2010) Long-term depression in the CNS. *Nat Rev Neurosci* **11**, 459-473
3. Manahan-Vaughan, D., and Braunewell, K. H. (1999) Novelty acquisition is associated with induction of hippocampal long-term depression. *P Natl Acad Sci USA* **96**, 8739-8744
4. Ge, Y., Dong, Z., Bagot, R. C., Howland, J. G., Phillips, A. G., Wong, T. P., and Wang, Y. T. (2010) Hippocampal long-term depression is required for the consolidation of spatial memory. *P Natl Acad Sci USA* **107**, 16697-16702
5. Liu, X., Gu, Q. H., Duan, K., and Li, Z. (2014) NMDA receptor-dependent LTD is required for consolidation but not acquisition of fear memory. *J Neurosci.* **34**, 8741-8748
6. Bear, M. F., and Malenka, R. C. (1994) Synaptic plasticity: LTP and LTD. *Curr Opin neurobiol* **4**, 389-399
7. Peineau, S., Taghibiglou, C., Bradley, C., Wong, T. P., Liu, L., Lu, J., Lo, E., Wu, D., Saule, E., Bouschet, T., Matthews, P., Isaac, J. T., Bortolotto, Z. A., Wang, Y. T., and Collingridge, G. L. (2007) LTP inhibits LTD in the hippocampus via regulation of GSK3beta. *Neuron* **53**, 703-717
8. Zhu, J. J., Qin, Y., Zhao, M., Van Aelst, L., and Malinow, R. (2002) Ras and Rap control AMPA receptor trafficking during synaptic plasticity. *Cell* **110**, 443-455
9. Jiao, S., and Li, Z. (2011) Nonapoptotic function of BAD and BAX in long-term depression of synaptic transmission. *Neuron* **70**, 758-772
10. Li, Z., Jo, J., Jia, J. M., Lo, S. C., Whitcomb, D. J., Jiao, S., Cho, K., and Sheng, M. (2010) Caspase-3 activation via mitochondria is required for long-term depression and AMPA receptor internalization. *Cell* **141**, 859-871
11. Campbell, D. S., and Holt, C. E. (2003) Apoptotic pathway and MAPKs differentially regulate chemotropic responses of retinal growth cones. *Neuron* **37**, 939-952
12. Huesmann, G. R., and Clayton, D. F. (2006) Dynamic role of postsynaptic caspase-3 and BIRC4 in zebra finch song-response habituation. *Neuron* **52**, 1061-1072
13. Hyman, B. T., and Yuan, J. (2012) Apoptotic and non-apoptotic roles of caspases in neuronal physiology and pathophysiology. *Nat Rev Neurosci* **13**, 395-406

14. Lo, S. C., Wang, Y., Weber, M., Larson, J. L., Scearce-Levie, K., and Sheng, M. (2015) Caspase-3 deficiency results in disrupted synaptic homeostasis and impaired attention control. *J Neurosci.* **35**, 2118-2132
15. Obexer, P., and Ausserlechner, M. J. (2014) X-linked inhibitor of apoptosis protein - a critical death resistance regulator and therapeutic target for personalized cancer therapy. *Front oncol* **4**, 197
16. Unsain, N., Higgins, J. M., Parker, K. N., Johnstone, A. D., and Barker, P. A. (2013) XIAP regulates caspase activity in degenerating axons. *Cell rep* **4**, 751-763
17. Harlin, H., Reffey, S. B., Duckett, C. S., Lindsten, T., and Thompson, C. B. (2001) Characterization of XIAP-deficient mice. *Mol cell biol* **21**, 3604-3608
18. Stellwagen, D., Beattie, E. C., Seo, J. Y., and Malenka, R. C. (2005) Differential regulation of AMPA receptor and GABA receptor trafficking by tumor necrosis factor-alpha. *J Neurosci* **25**, 3219-3228
19. Kaech, S., and Banker, G. (2006) Culturing hippocampal neurons. *Nat protoc* **1**, 2406-2415
20. Erturk, A., Wang, Y., and Sheng, M. (2014) Local pruning of dendrites and spines by caspase-3-dependent and proteasome-limited mechanisms. *J Neurosci* **34**, 1672-1688
21. Hasegawa, S., Sakuragi, S., Tominaga-Yoshino, K., and Ogura, A. (2015) Dendritic spine dynamics leading to spine elimination after repeated inductions of LTD. *Sci rep* **5**, 7707
22. Nagerl, U. V., Eberhorn, N., Cambridge, S. B., and Bonhoeffer, T. (2004) Bidirectional activity-dependent morphological plasticity in hippocampal neurons. *Neuron* **44**, 759-767
23. Zhou, Q., Homma, K. J., and Poo, M. M. (2004) Shrinkage of dendritic spines associated with long-term depression of hippocampal synapses. *Neuron* **44**, 749-757
24. Sun, C., Cai, M., Gunasekera, A. H., Meadows, R. P., Wang, H., Chen, J., Zhang, H., Wu, W., Xu, N., Ng, S. C., and Fesik, S. W. (1999) NMR structure and mutagenesis of the inhibitor-of-apoptosis protein XIAP. *Nature* **401**, 818-822
25. Riedl, S. J., Renatus, M., Schwarzenbacher, R., Zhou, Q., Sun, C., Fesik, S. W., Liddington, R. C., and Salvesen, G. S. (2001) Structural basis for the inhibition of caspase-3 by XIAP. *Cell* **104**, 791-800
26. Sun, C., Cai, M., Meadows, R. P., Xu, N., Gunasekera, A. H., Herrmann, J., Wu, J. C., and Fesik, S. W. (2000) NMR structure and mutagenesis of the third Bir domain of the inhibitor of apoptosis protein XIAP. *J biol chem***275**, 33777-33781

27. Scott, F. L., Denault, J. B., Riedl, S. J., Shin, H., Renatus, M., and Salvesen, G. S. (2005) XIAP inhibits caspase-3 and -7 using two binding sites: evolutionarily conserved mechanism of IAPs. *EMBO j* **24**, 645-655

28. Lopez, J., and Meier, P. (2010) To fight or die - inhibitor of apoptosis proteins at the crossroad of innate immunity and death. *Curr opin cell biol* **22**, 872-881

29. Unsain, N., and Barker, P. A. (2015) New Views on the Misconstrued: Executioner Caspases and Their Diverse Non-apoptotic Roles. *Neuron* **88**, 461-474

Figure Legends

Figure 1. Deletion of XIAP enhances LTD

(A) The presence of XIAP and caspase-3 was determined in synaptosomal fractions from adult WT and XIAP$^{-/-}$ brains (H: Homogenate S: Synaptosomes). (**B)** Hippocampal slices were subjected to low frequency stimulation (LFS, 15 minutes, 1Hz) to induce LTD. Insets show representative field recordings traces of eEPSC at the indicated times during recording. Numbers in brackets depicts number of slices used. (**C)** Hippocampal slices from WT and XIAP$^{-/-}$ treated for 2 h with zDEVD-fmk (2 μM) were subjected to low frequency stimulation (LFS) to induce LTD. Insets show representative traces of eEPSC during recording. Numbers in brackets depicts number of slices used. (**D)** Identical LTD protocol as in (**B)** but with slices from WT, CASP3$^{-/-}$ and CASP3$^{-/-}$ :: XIAP$^{-/-}$ mice.

Figure 2. Deletion of XIAP enhances level of active caspase 3

Hippocampal neurons from WT and XIAP$^{-/-}$ were maintained on porous filters for 15 days and then treated with NMDA. (**A)** The bottom side of filters containing axons and dendrites but devoid of cell bodies was collected and subjected to biotin-VAD pull down to detect active caspases. (**B)** Quantification of active caspase-3 level in each condition (n = 4 experiments).

Figure 3. Deletion of XIAP reduces the number of synapses

(A) Representative staining of hippocampal neurons maintained in culture 21 days stained for MAP2 (blue), PSD95 (green) and synapsin-1 (red), magnified in (**B)**.

(C) Quantification of synapse density, p = 0.012, n = 3 independent experiments.

Figure 4. Deletion of XIAP alters synaptic activity

(A) Representative mEPSC recorded in hippocampal slices (n = 6 slices/genotype). (**B)** Cumulative probability plots for amplitude and inter-event intervals (IEI, **C**) of mEPSCs reveal significant differences between genotypes (KS-test). (**D)** Hippocampal slices from WT and XIAP$^{-/-}$ mice were subject to paired-pulse facilitation measurements using 20 to 500 ms between pulses. No differences between WT and XIAP$^{-/-}$ were observed (n = 7 slices/genotype).

Figure 5. Deletion of XIAP increases AMPA internalization after NMDA treatment

(A) Representative GluR2 staining before and after NMDA treatment of hippocampal neurons from WT and XIAP$^{-/-}$ mice. (**B)** Quantification of GluR2 internalization. For each channel the mean intensity per image including neuronal somata was measured and the ratio of internalized/ surface

GluR2 signal was calculated (n = 137 images for WT, n = 151 images for WT + NMDA, n = 138 images for $XIAP^{-/-}$ and n = 140 images for $XIAP^{-/-}$ + NMDA from 5 independent cultures) *p < 0.05, **p < 0.01, ***p < 0.001 One-way ANOVA follow by a Bonferroni's Multiple Comparison Test.

Figure 6 Deletion of XIAP accelerates learning in novel object location and fear extinction tasks.

(A) Comparison of wild-type versus $XIAP^{-/-}$ mice in motor learning on a Rotarod. (**B)** The same mice were tested for anxiety in an open field. (**C)** Exploration time during training of a novel object location task. **(D)** Percentage of novel object exploration in training sessions #2, #3 and #4. Statistical analysis performed was one-way ANOVA. (**E)** Novel object location preference score 24h after the last session of learning and (**F)** total exploration time at day 5. (**G)** Contextual fear extinction learning and retention test. Freezing curves during extinction sessions reveal faster extinction in $XIAP^{-/-}$ mice than controls, but no differences when tested 24h later. Data points represent means +/- SEM.

Figure 1

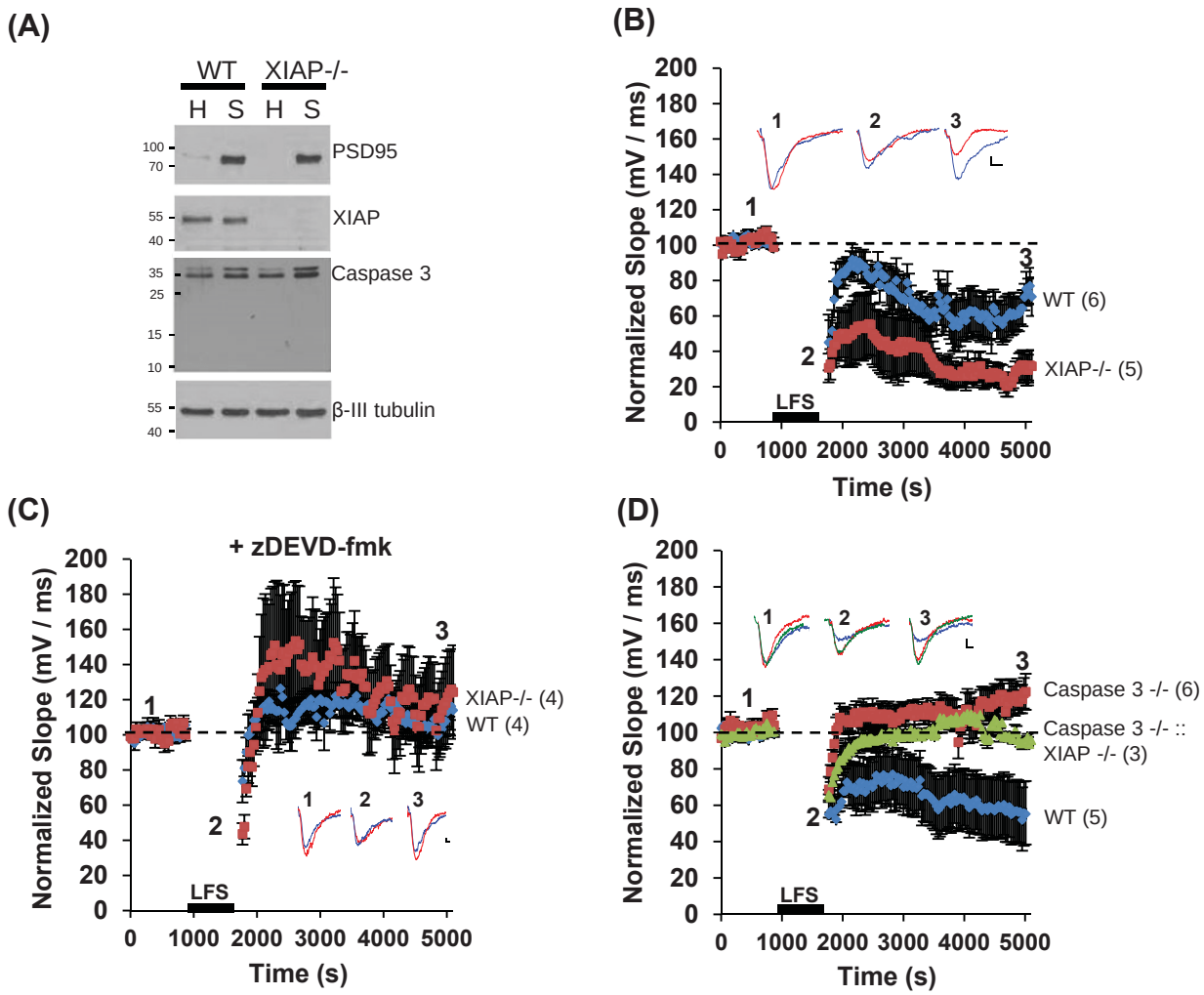
(A)
WT
XIAP-/-
H S H S
100
70
PSD95
55
40
XIAP
35
25
15
10
Caspase 3
55
40
β-III tubulin
(B)
Normalized Slope (mV / ms)
Time (s)
LFS
WT (6)
XIAP-/- (5)
(C)
+ zDEVD-fmk
XIAP-/- (4)
WT (4)
(D)
Caspase 3 -/- (6)
Caspase 3 -/- ::
XIAP -/- (3)
WT (5)

Figure 2

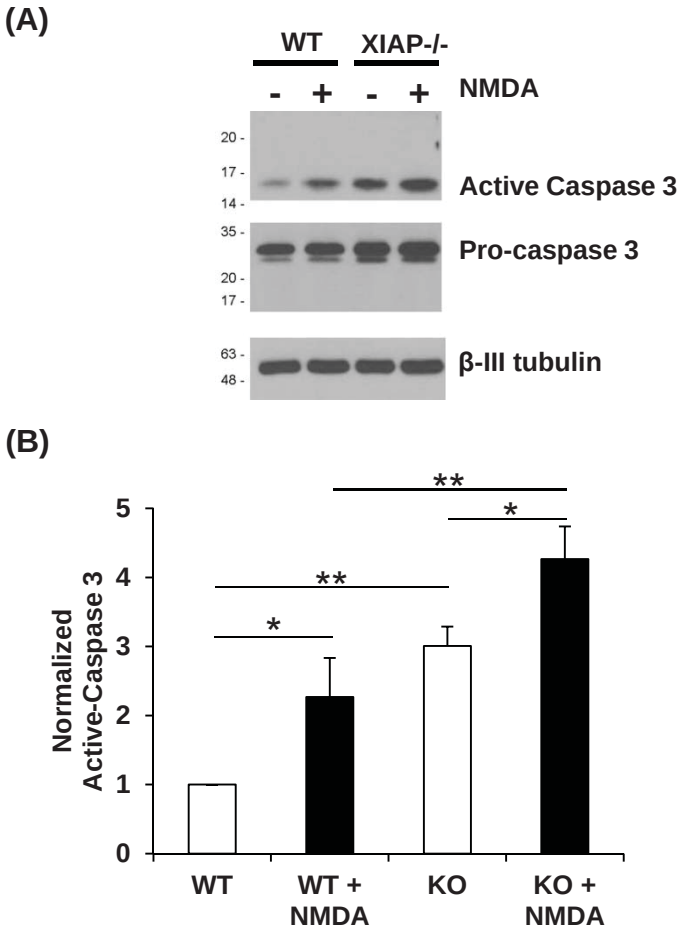
(A)
WT
XIAP-/-
- + - +
NMDA
20 -
17 -
14 -
Active Caspase 3
35 -
20 -
17 -
Pro-caspase 3
63 -
48 -
β-III tubulin
(B)
Normalized Active-Caspase 3
0
1
2
3
4
5
**
*
**
*
WT
WT + NMDA
KO
KO + NMDA

Figure 3

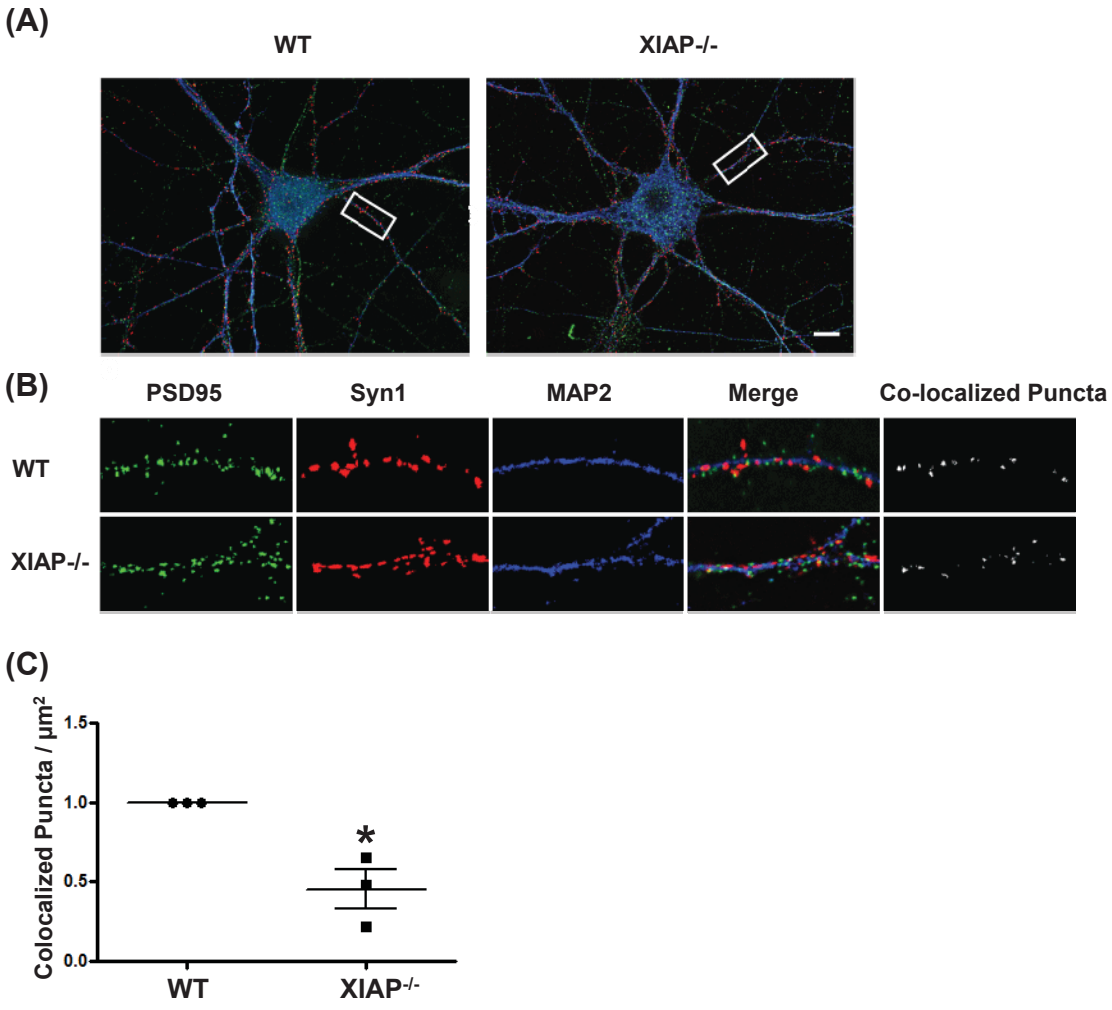
(A)
WT
XIAP-/-
(B)
PSD95
Syn1
MAP2
Merge
Co-localized Puncta
WT
XIAP-/-
(C)
Colocalized Puncta / µm²
1.5
1.0
0.5
0.0
*
WT
XIAP-/-

Figure 4

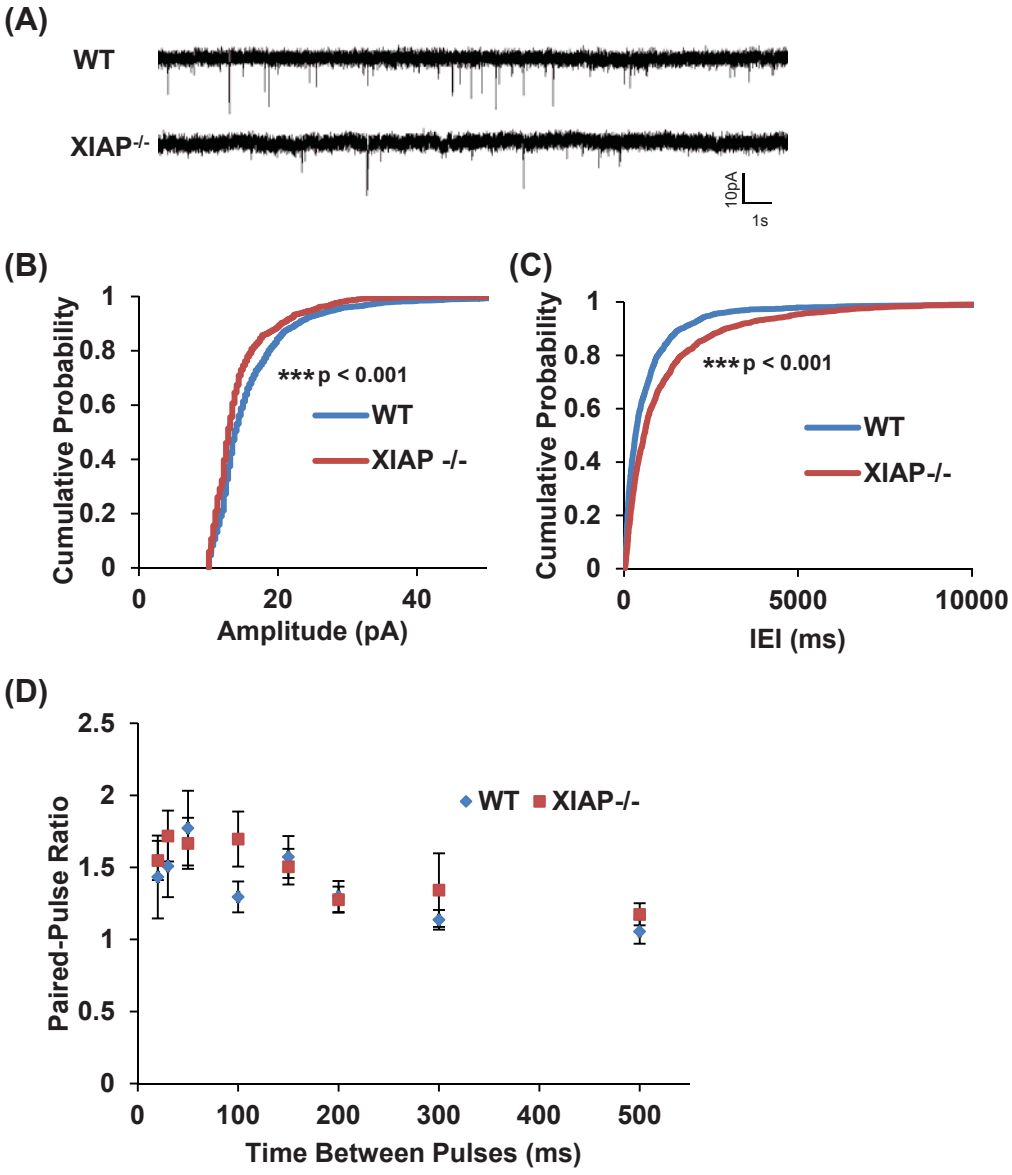
(A)
WT
XIAP-/-
10pA
1s
(B)
Cumulative Probability
*** p < 0.001
WT
XIAP -/-
Amplitude (pA)
(C)
Cumulative Probability
*** p < 0.001
WT
XIAP-/-
IEI (ms)
(D)
Paired-Pulse Ratio
WT
XIAP-/-
Time Between Pulses (ms)

Figure 5

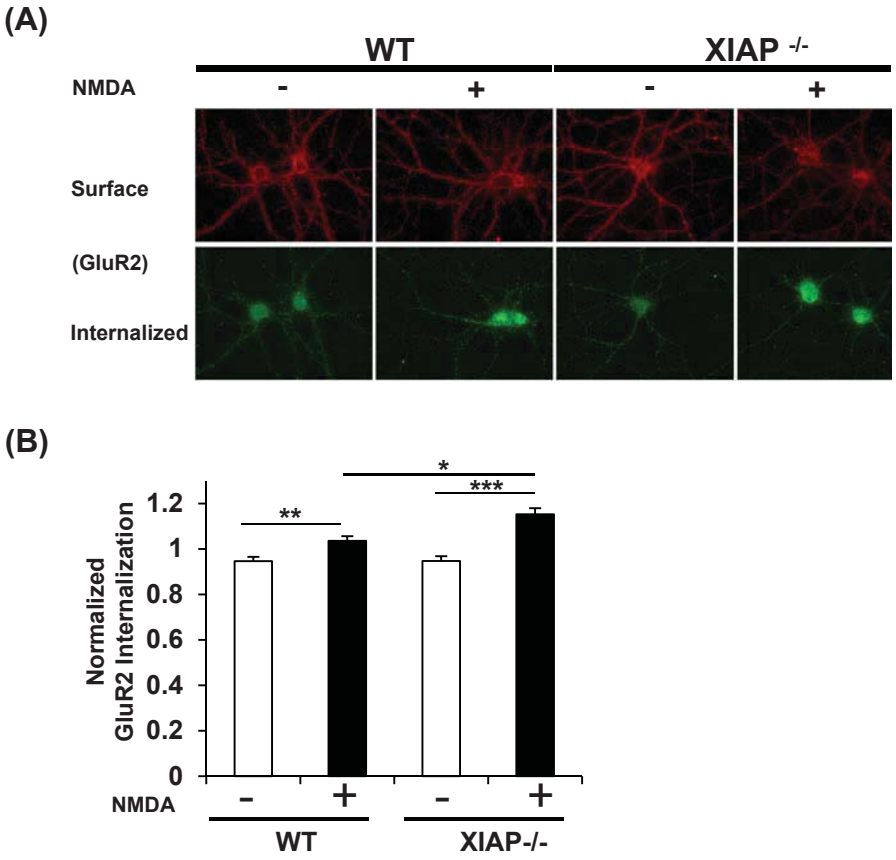
(A)
WT
XIAP -/-
NMDA
-
+
-
+
Surface
(GluR2)
Internalized
(B)
Normalized GluR2 Internalization
1.2
1
0.8
0.6
0.4
0.2
0
**
*
***
NMDA
-
+
-
+
WT
XIAP-/-

Figure 6

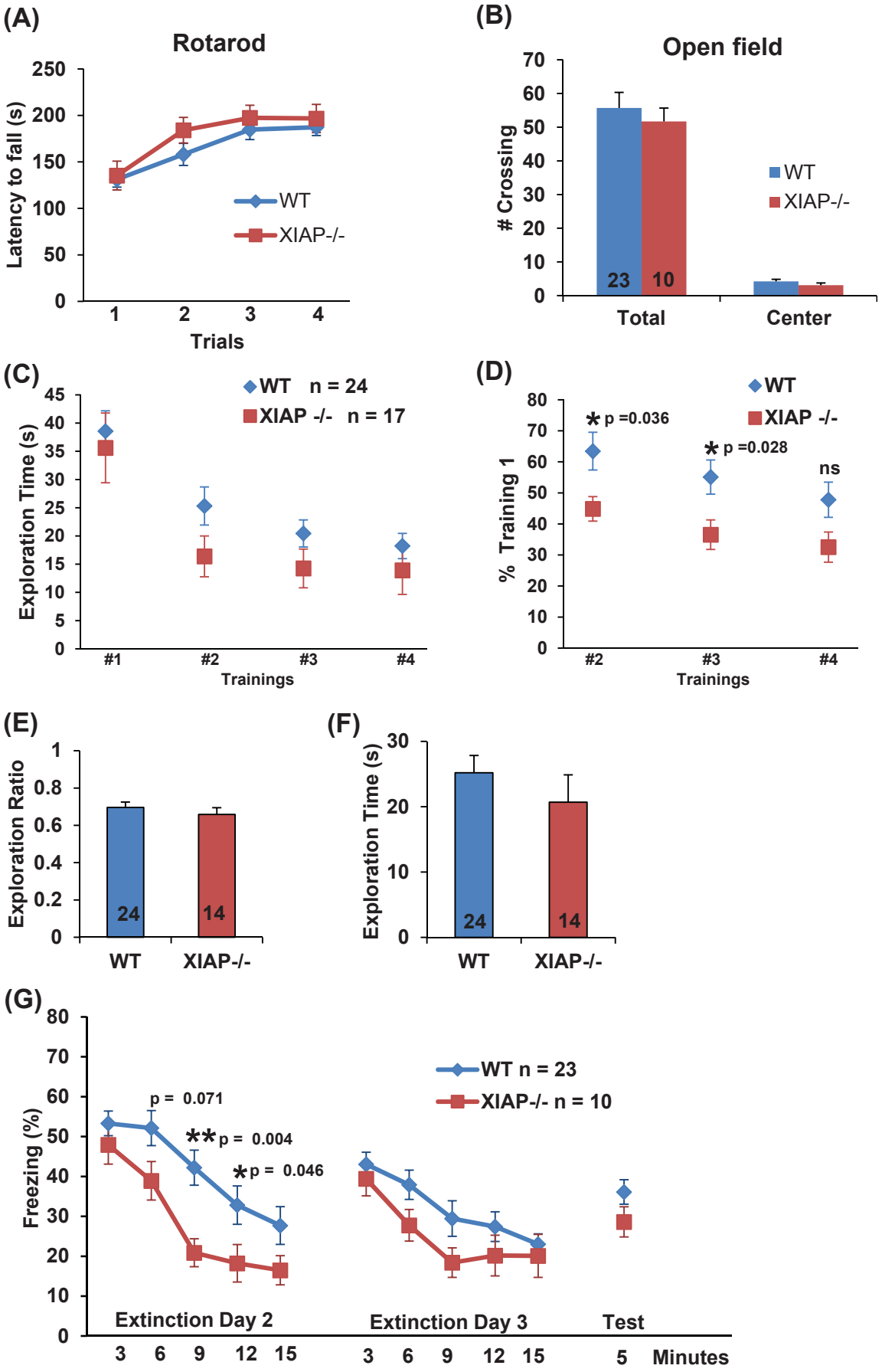
(A)
Rotarod
Latency to fall (s)
250
200
150
100
50
0
1
2
3
4
Trials
WT
XIAP-/-
(B)
Open field
Crossing
70
60
50
40
30
20
10
0
23
10
Total
Center
WT
XIAP-/-
(C)
WT n = 24
XIAP -/- n = 17
Exploration Time (s)
45
40
35
30
25
20
15
10
5
0
#1
#2
#3
#4
Trainings
(D)
WT
XIAP -/-
* p =0.036
* p =0.028
ns
% Training 1
80
70
60
50
40
30
20
10
0
#2
#3
#4
Trainings
(E)
Exploration Ratio
1
0.8
0.6
0.4
0.2
0
24
14
WT
XIAP-/-
(F)
Exploration Time (s)
30
20
10
0
24
14
WT
XIAP-/-
(G)
Freezing (%)
80
70
60
50
40
30
20
10
0
p = 0.071
** p = 0.004
* p = 0.046
WT n = 23
XIAP-/- n = 10
Extinction Day 2
Extinction Day 3
Test
3
6
9
12
15
3
6
9
12
15
5
Minutes